Chapter 11
A Novel Underwater Image Enhancement Approach with Wavelet Transform Supported by Differential Evolution Algorithm

Gur Emre Guraksin, Omer Deperlioglu and Utku Kose

Abstract In this paper, a novel underwater image enhancement approach was proposed. This approach includes use of a method formed by the wavelet transform and the differential evolution algorithm. In the method, the contrast adjustment function was applied to the original underwater image first. Then, the homomorphic filtering technique was used to normalize the brightness in the image. After these steps, the underwater image was separated into its R, G, and B components. Then wavelet transform function was performed on each of the R, G, and B channels with Haar wavelet decomposition. Thus, detailed images were obtained for each of the color channels by wavelet transform low-pass approximation (cA), horizontal (cH), vertical (cV) and diagonal (cD) coefficients. Four parameters of weights (w) of each component cA, cH, cV, and cD situated in the R, G, and B color channels were optimized using differential evolution algorithm. In the proposed method, differential evolution algorithm was employed to find the optimum w parameters for Entropy and PSNR in separate approaches. Finally, unsharp mask filter was used to enhance the edges in the image. As an evaluation approach, performance of the proposed method was tested by using the criteria of entropy, PSNR, and MSE. The obtained results showed that the effectiveness of the proposed method was better than the existing techniques. Likewise, the visual quality of the image was also improved more thanks to the proposed method.

G. E. Guraksin
Department of Biomedical Engineering, Afyon Kocatepe University, Afyonkarahisar, Turkey
e-mail: emreguraksin@aku.edu.tr

O. Deperlioglu
Department of Computer Technologies, Afyon Kocatepe University, Afyonkarahisar, Turkey
e-mail: deperlioglu@aku.edu.tr

U. Kose (✉)
Department of Computer Engineering, Suleyman Demirel University, Isparta, Turkey
e-mail: utkukose@sdu.edu.tr

J. Hemanth and V. E. Balas (eds.), *Nature Inspired Optimization Techniques for Image Processing Applications*, Intelligent Systems Reference Library 150,
https://doi.org/10.1007/978-3-319-96002-9_11

Keywords Underwater image enhancement · Differential evolution algorithm Wavelet transform · Optimization · Artificial intelligence

11.1 Introduction

The physical properties of water have the disruptive effects on taking an underwater image such as the attenuation of light, absorption and scattering of light, and the foggy environment. For this reason, underwater images have poor color quality and low visibility, and also one color dominates on underwater image. To overcome these problems, underwater image enhancement has an important role for underwater scientists. There are several proposed methods or approaches in the literature such as contrast enhancement, the optical priors, fusion, and dehazing etc. for overcoming the problems related to underwater imaging [1–5].

The underwater image processing generally contains two different methods which are the image restoration and the image enhancement methods. The image restoration method aims to recover a row image using a model of reduction and model of original image configuration. These methods are meticulous and very powerful. But, these methods comprise a plurality of variables and parameters [6]. The image enhancement methods use the qualitative subjective criteria of image. But to achieve a more visually pleasing image, they do not need any physical model for image formation. In this context, such methods are usually faster and simpler deconvolution approaches [7]. When we take a look at the related literature, it can be seen that there are many different methods employed in order to achieve enhancement of underwater images [8–15].

Preprocessing techniques have a great importance for the underwater image enhancement methods. Therefore, many researchers developed several preprocessing methods for underwater image enhancement. Sometimes, the filter methods were used alone or with different methods and also sometimes a few filters were used together with other filters [16–19]. For example, Bazeille et al. proposed an automatic method to pre-process underwater images. It reduced underwater perturbations and improved image quality. This method did not require any parameter setting. The method proposed by Bazeille et al. was used as a first process of edge detection. The robustness of the method was analyzed using an edge detection robustness criterion [20].

One of the most supportive improvement activities of the underwater image improvement is artificial intelligence or optimization algorithms such as fuzzy logic, Vortex Optimization Algorithm and Constancy Deskewing Algorithm etc. [3, 4, 21, 22]. Ratna Babu and Sunitha proposed an image enhancement approach based on Cuckoo Search Algorithm with Morphological Operations. First, they selected the best contrast value of an image with Cuckoo Search algorithm. Then, they carried out morphological operations. From the obtained results, they said that "the proposed approach is converted into original color image without noise and adaptive process enhance the quality of images" [23].

Nowadays, the wavelet transform is a very popular method of underwater processing. Usually, it is used in very different ways for image compression and removing noise [2, 24]. Discrete Wavelet Transforms (Haar, Daubechies, etc.) are orthogonal wavelet, and their forward and inverse transforms require only additions and subtractions. Therefore, implementing these functions on the computer are very easy. Today, one of the most favorable techniques is the Discrete Wavelet Transform which uses the Haar functions in image coding, edge extraction and binary logic design [25].

In this paper, a new approach for the underwater images enhancement was proposed. This method contain wavelet transform and differential evolution algorithm. Differential evolution algorithm is one of the most powerful optimization algorithms as having the advantages of evolutionary approaches, requiring less parameter setting, and being efficient on complex optimization problems even though it has a simple structure [26–28]. On the other hand, wavelet transform is a powerful, multidisciplinary technique used widely for solving difficult problems in different fields like mathematics, physics, and engineering by focusing on applications such as signal processing, image processing, data compression, and pattern recognition [29, 30]. Wavelet transform is better than the traditional Fourier methods with its advantages on employing localized basis functions and achieving faster computation [31]. Because of remarkable advantages of these techniques, the authors decided to combine them for the research problem of this study.

Regarding the subject of the paper and the performed research, remaining content was organized as follows: In the second section, wavelet transform, differential evolution algorithm, contrast adjustment, homomorphic filter, and unsharp mask filter were described in details. Following to that, findings obtained from the performed applications on underwater image enhancement and also a general discussion on them were given in the third section. Then, the paper was ended with the last section providing explanations on conclusions and some possible future works.

11.2 Theoretical Background

Just before focusing on the applications on underwater image enhancement, it is important to give brief information about theoretical background regarding the followed enhancement approach. The following subtitled were devoted to that purpose.

11.2.1 Wavelet Transform

When X represents an indexed image, X as well as the output arrays cA, cH, cV, and cD are m-by-n matrices. When X represents a true color image, it is an m-by-n-by-3 array, where each m-by-n matrix represents a red, green, or blue color

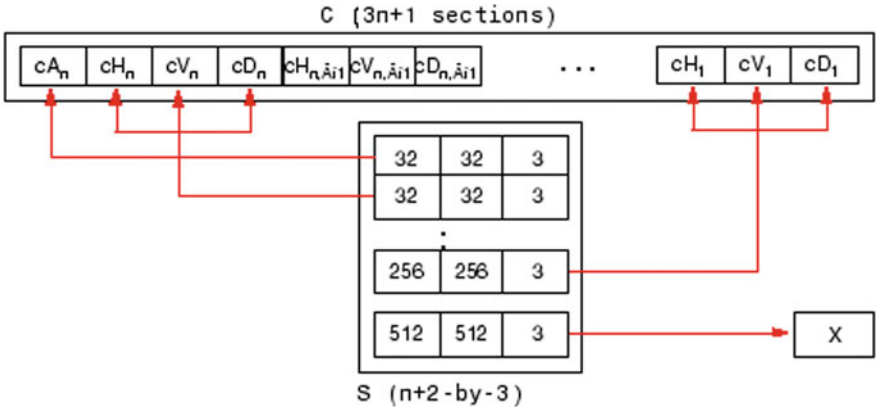

Fig. 11.1 The decomposition vector C and the corresponding bookkeeping matrix S [32]

plane concatenated along the third dimension. The size of vector C and the size of matrix S depend on the type of analyzed image. For a true color image, the decomposition vector C and the corresponding bookkeeping matrix S can be represented as in Fig. 11.1 [32].

For images, the wavelet representation can be computed with a pyramidal algorithm similar to the one-dimensional algorithm for two-dimensional wavelets and scaling functions. A two-dimensional wavelet transform can be computed with a separable extension of the one-dimensional decomposition algorithm. At each step, we decompose $A^d_{2^{j+1}}f$ into $A^d_{2^j}f$, $D^1_{2^j}f$, $D^2_{2^j}f$, and $D^3_{2^j}f$. This algorithm is shown as a block diagram in Fig. 11.2. Firstly, the rows of $A^d_{2^{j+1}}f$ are convolved with a one-dimensional filter, retain every other row. Then the columns of the resulting signals are convolved with another one-dimensional filter and retain every other column. The filters used in this decomposition are the quadrature mirror filters $\hat{H}$ and $\hat{G}$. The structure of application of the filters for computing $A^d_{2^j}$, $D^1_{2^j}$, $D^2_{2^j}$, and $D^3_{2^j}$ are shown in Fig. 11.2 [32]. The wavelet transform of an image is computed $A^d_1 f$ by repeating this process for $-1 \geq j \geq -J$. This corresponds to a separable conjugate mirror filter decomposition [32, 33].

Let us use an orthogonal wavelet for the computation scheme which becomes easy. We start with the two filters of length 2N, denoted h(n) and g(n) and corresponding to the wavelet. Now by induction, let us define the following sequence of functions (Wn (x), n = 0, 1, 2, 3, …) as Eqs. 11.1 and 11.2:

$$W_{2n}(x) = \sqrt{2} \sum_{k=0,\cdots,2N-1} h(k) W_n(2x-k) \tag{11.1}$$

$$W_{2n+1}(x) = \sqrt{2} \sum_{k=0,\cdots,2N-1} g(k) W_n(2x-k) \tag{11.2}$$

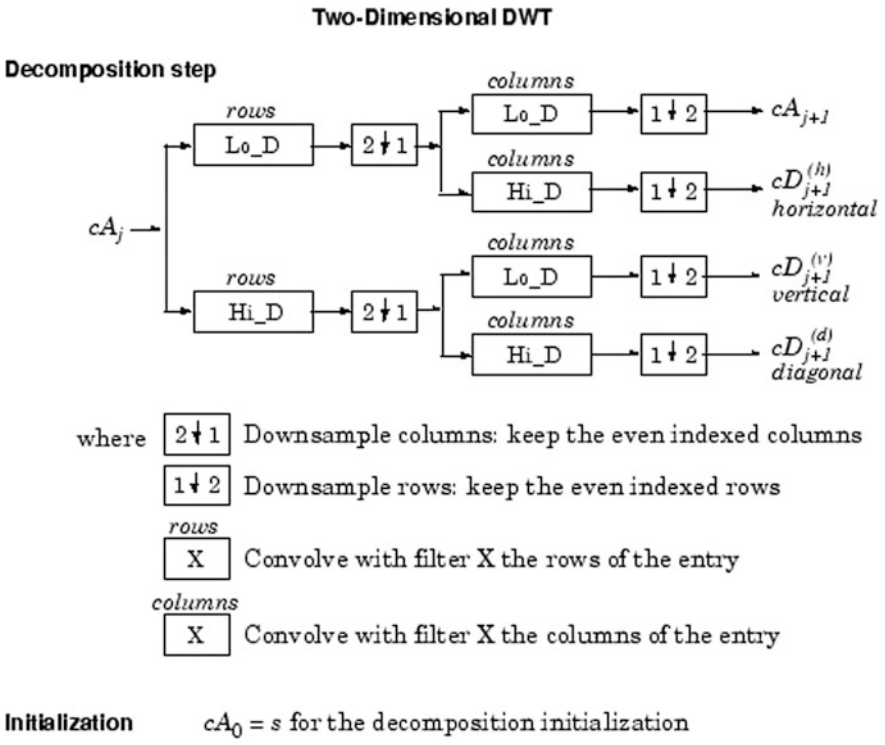

Fig. 11.2 Two-dimensional decomposition of an image [32]

where W0(x) = ϕ(x) is the scaling function and W1(x) = ψ(x) is the wavelet function [32].

The original Haar definition is as Eq. 11.3:

$$haar(0,t) = 1, \quad for\, t \in [0,1); \quad haar(1,t) = \begin{cases} 1, & for\, t \in \left[0, \frac{1}{2}\right), \\ -1, & for\, t \in \left[\frac{1}{2}, 1\right) \end{cases} \tag{11.3}$$

and $haar(k,0) = \lim_{t \to 0} + haar(k,t)$, $haar(k,1) = \lim_{t \to 1} + haar(k,t)$ and at the points of discontinuity within the interior (0, 1) $haar(k,t) = \frac{1}{2}(haar(k,t-0) + haar(k,t+0))$ [25].

For the Haar wavelet, Eqs. 11.1 and 11.2 are transformed into Eqs. 11.6 and 11.7, respectively:

$$N = 1, \quad h(0) = h(1) = \frac{1}{\sqrt{2}} \tag{11.4}$$

$$g(0) = g(1) = \frac{1}{\sqrt{2}} \tag{11.5}$$

$$W_{2n}(x) = W_n(2x) + W_n(2x-1) \tag{11.6}$$

$$W_{2n+1}(x) = W_n(2x) - W_n(2x-1) \tag{11.7}$$

$W_0(x) = \phi(x)$ is the haar scaling function and $W_1(x) = \psi(x)$ is the Haar wavelet, both supported in [0, 1]. So W_{2n} can be obtained by adding two 1/2-scaled versions of W_n with distinct support intervals. W_{2n+1} can be obtained by subtracting the same versions of W_n. Starting from more regular original wavelets, using a similar construction, the smoothed version of this system of W-functions is obtained all with support in the interval [0, 2N − 1] [32].

11.2.2 Differential Evolution Algorithm

The Differential Evolution Algorithm (DEA) is an artificial intelligence based on optimization algorithm introduced by Storn and Price in 1997 [28, 34, 35]. The DEA is a stochastic search technique based on population for solving global optimization problems. This algorithm is very simple but powerful, and the algorithm efficiency and effectiveness have been proven in many different applications [26, 36–42].

At first, the DEA starts with the population of Np, and D-dimension vectors with parameter values, which are randomly and uniformly distributed between the pre-specified lower initial parameter bound x_j, low and the upper initial parameter bound x_j, high:

$$x_{j,i,G} = x_{j,low} + rand(0,1).(x_{j,high} - x_{j,low}), \quad j = 1,2,\ldots,D; \quad i = 1,2,\ldots,N_p; \quad G = 0 \tag{11.8}$$

In Eq. 11.8, G is the generation index to which the population belongs, index i represents the ith solution of population index, and j indicates the parameter index.

The DEA has three main solution mechanisms as mutation, crossover, and selection. Thanks to these mechanisms, the DEA is known as an evolutionary solution approach (So, it also has the word “evolution” in its name) [43–45]. In detail, Khan et al. expressed pseudo code of the DEA as in Fig. 11.3 [46]. For more examples of pseudo code, readers are referred to [47, 48].

Figure 11.4 provides a brief flow chart of the DAE [49].

With its wide use, the DAE has also had many different modified versions in the related literature and in this way, it has been used along a wide scope of research problems [50–56].

Generate the initial population of individuals
Do
For each individual j in the population
Choose three numbers $n_1, n_2,$ *and* n_3 *that is,* $1 \le n_1, n_2, n_3 \le N$ *with* $n_1 \ne n_2 \ne n_3 \ne j$
Generate a random integer $i_{\text{rand}} \in (1, N)$
For each parameter i

$$y^{i,g} = x^{n_1,g} + F(x^{n_2,g} - x^{n_3,g})$$

$$z_j^{i,g} = \begin{cases} y_j^{i,g} if \text{ rand}() \le \text{CR } or \ j = j_{\text{rand}} \\ x_j^{i,g} \text{otherwise} \end{cases}$$

End For
Replace $x^{i,g}$ *with the child* $z^{i,g}$ *if* $z^{i,g}$ *is better*
End For
Until the termination condition is achieved

Fig. 11.3 A pseudo code of the DEA [46]

11.2.3 Contrast Adjustment

The most primary way of image processing is point transform. It means that this transform maps the values at individual pixels in the input image into corresponding pixels in an output image. In the mathematical concept, this is a one-to-one functional mapping from input to output, arithmetic or logical operations on images. These operations can be applied between two images, IA and IB, or can be applied between an image IA and a constant C. For example, Iout = IA + IB or Iout = IA + C.

Contrast adjustment is a method obtained by adding or multiplying a positive constant value C to each pixel location. This operation increases pixel's value and pixel's brightness. In general, it is a multiplier. For the color image, firstly, the color image is separated into its R, G, and B components. Then, contrast adjustment is applied for each R, G, and B components separately [57].

11.2.4 Homomorphic Filter

When the illumination-reflectance model is considered, it is supposed that an image is a function of the product of the illumination and the reflectance as described in Eq. 11.9:

$$f(x, y) = i(x, y) \cdot r(x, y) \tag{11.9}$$

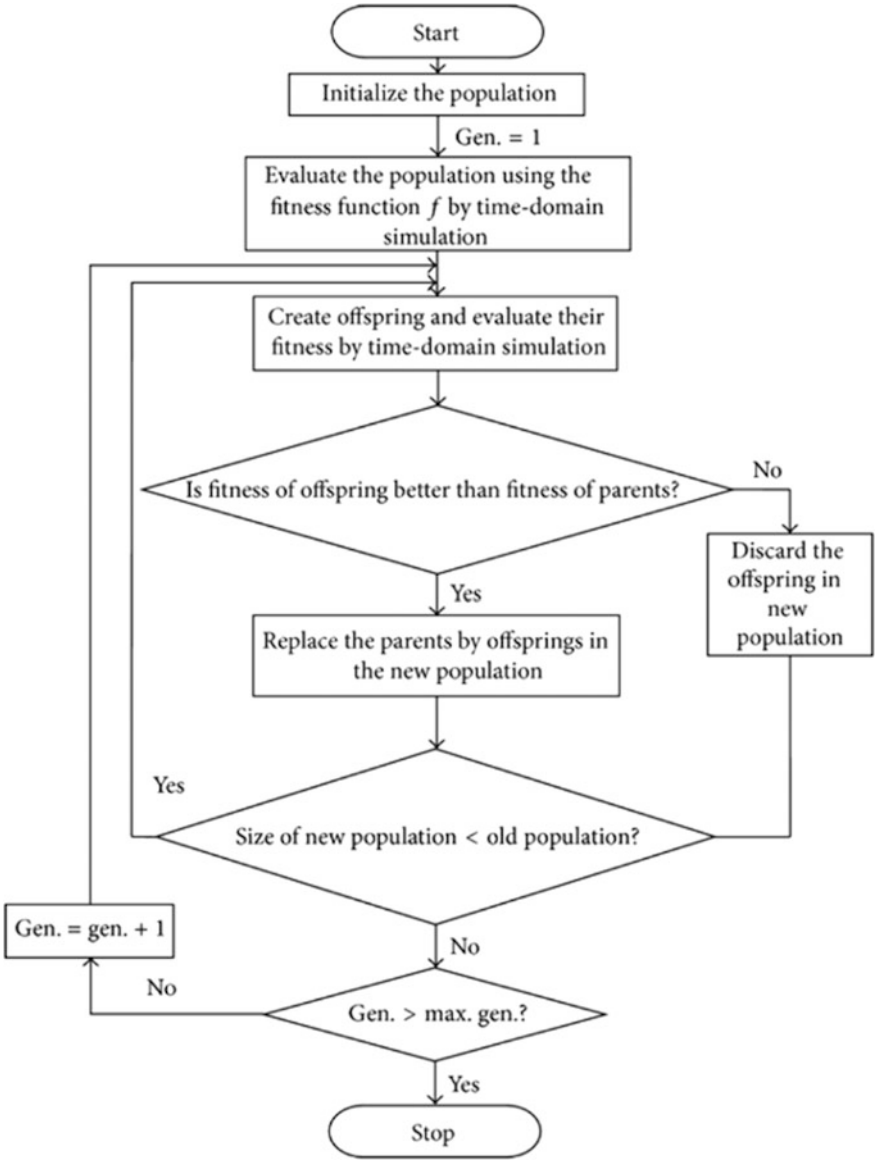

Fig. 11.4 A brief flow chart of the DAE [49]

where f(x, y) is the input image, i(x, y) is the illumination multiplicative factor, and r(x, y) is the reflectance function. In this context, the illumination factor changes slowly through the view field, therefore it represents low frequencies in the Fourier transform of the image. On the contrary, reflectance is associated with high frequency components. The low frequencies can be suppressed with a high-pass filter

by multiplying these components. Processes of the algorithm can be discussed step by step as follows:

- As seen in Eq. 11.10, the logarithm is taken to separate components of the illumination and reflectance. Thus, the multiplicative effect is converted into an additive one by the logarithm.

$$g(x,y) = \ln(f(x,y)) = \ln(i(x,y).r(x,y)) + \ln(r(x,y)) \tag{11.10}$$

- Equation 11.11 shows that the computation of the Fourier transform of the log-image.

$$G(w_x, w_y) = I(w_x, w_y) + R(w_x, w_y) \tag{11.11}$$

- Equation 11.12 shows that the high-pass filter applied to the Fourier transform decreases the contribution of illumination and also amplifies the contribution of reflectance. Thus, the edges of the objects in the image is sharpened.

$$\begin{aligned} &S(w_x, w_y) = H(w_x, w_y) \cdot I(w_x, w_y) + H(w_x, w_y) \cdot R(w_x, w_y) \\ &with, \quad H(w_x, w_y) = (r_H - r_L) \cdot (1 - \exp(-(\frac{w_x^2 + w_y^2}{2\delta_w^2}))) + r_L \end{aligned} \tag{11.12}$$

where $r_H = 2.5$ and $r_L = 0.5$ are the maximum and minimum coefficients values respectively, and δ_w is the factor controlling the cutoff frequency. These parameters are selected empirically [20].

Computation of the inverse Fourier transform is used to come back in the spatial domain and then taking the exponent to obtain the filtered image [20].

11.2.5 Unsharp Masking

The unsharp mask filter is an edge enhancement filter and it is also called as boost filtering. Unsharp filtering works by taking a smoothed version of an image obtained from the original image in order to improve the high-frequency information in the image. Firstly, this function generates an edge image from the original image using Eq. 11.13:

$$I_{edges}(c,r) = I_{original}(c,r) - I_{smoothed}(c,r) \tag{11.13}$$

The smoothed version of the image is generally obtained from filtering the original image with a kernel of a mean or a Gaussian filter. Then, the resulting difference image is added on to the original image to carry out some degree of sharpening as given in Eq. 11.14:

$$I_{enhanced}(c,r) = I_{original}(c,r) + k(I_{edges}(c,r)) \tag{11.14}$$

where the constant scaling factor k is used to ensure the resulting image to be within the proper range. Generally, k can be selected between 0.2 and 0.7 depending on the level of required sharpening. The operation here is called sometimes as boost filtering [57].

11.3 Solution of the Proposed Image Enhancement Approach

In this paper, we proposed a new approach to enhance the underwater images using wavelet transform and differential evolution algorithm. In the first stage of the proposed technique, contrast adjustment procedure was applied to the original underwater image. By the help of this procedure, we adjusted the contrast in the image with the limits of 0.01 and 0.99, so the contrast of the output image was increased. After the contrast adjustment procedure, homomorphic filtering procedure was used to normalize the brightness in the image which is a generalized technique for nonlinear image enhancement and correction. In the next stage the underwater image was separated into its R, G, and B components. Then wavelet transform operation was performed to each R, G, and B channels. For this purpose, the Haar wavelet decomposition was used. Thus, by the help of wavelet transform, lowpass approximation (cA), horizontal (cH), vertical (cV) and diagonal (cD) detailed images were obtained for each color channels. In this part of the algorithm, a weight value for each of the components (totally four weight value) obtained by wavelet transform was assigned by the help of the differential evaluation algorithm. Using the differential evolution algorithm, we optimized these four weight (w) parameters of each component cA, cH, cV and cD residing in the R, G and B color channels.

In the proposed approach, the differential evolution algorithm was employed to find the optimum w parameter maximizing the sum of the entropy of the reconstructed image. Besides, the entropy of the improved image, PSNR, and sum of Entropy and PSNR were also used as fitness function to find the optimum w parameter in the differential evolution algorithm. While using the differential evolution algorithm, there are some parameters like population size (N), length of the chromosome (D), the mutation factor (F), the crossover rate (C), and the maximum generations number (g) in the algorithm which must be initialized at first. These are the main parameters of the differential evolution algorithm. In this study, we supposed that N = 40, F = 0.8, C = 0.8, and g = 1000. Also, as we had four parameters for optimization, the length of a chromosome (D) was four. During the initialization of the population, the w parameters were randomly selected between 0 and 1. The fitness function was employed as the entropy (also we tried PSNR and sum of the entropy and PSNR) of the generated image pointing the richness of

information in the image. After the weighting procedure of the wavelet components finished, the new R, G, and B components were obtained by reconstructing the wavelet coefficients. In the next stage of the algorithm, unsharp masking procedure was used to enhance the edges in the image. By the help of unsharp masking, an enhanced version of the image (in which some features such as edges were sharpened) was obtained. A detailed solution flow of the proposed enhancement approach is given in Fig. 11.5.

In Fig. 11.6, an example process for an image by the proposed enhancement approach is given. Briefly, the first image (a) represents the original underwater image. In the second stage: (b), contrast adjustment procedure was applied to the original underwater image. After contrast adjustment procedure, homomorphic filtering operation (c) applied version of the image is given in the third image. In the fourth step of the system (d) filtered image was separated into its R, G and B color components. After that, by the help of wavelet transform lowpass approximation (cA), horizontal (cH), vertical (cV) and diagonal (cD) detailed images were obtained for each color channels and weighting procedure was applied to these color channels. So the new R, G and B color components (e) was obtained. In the sixth image (f), weighting R, G and B components was fused and the new color image was obtained. At the last step (g) unsharp masking procedure was applied to the new colored image and the enhanced version of the underwater image was obtained.

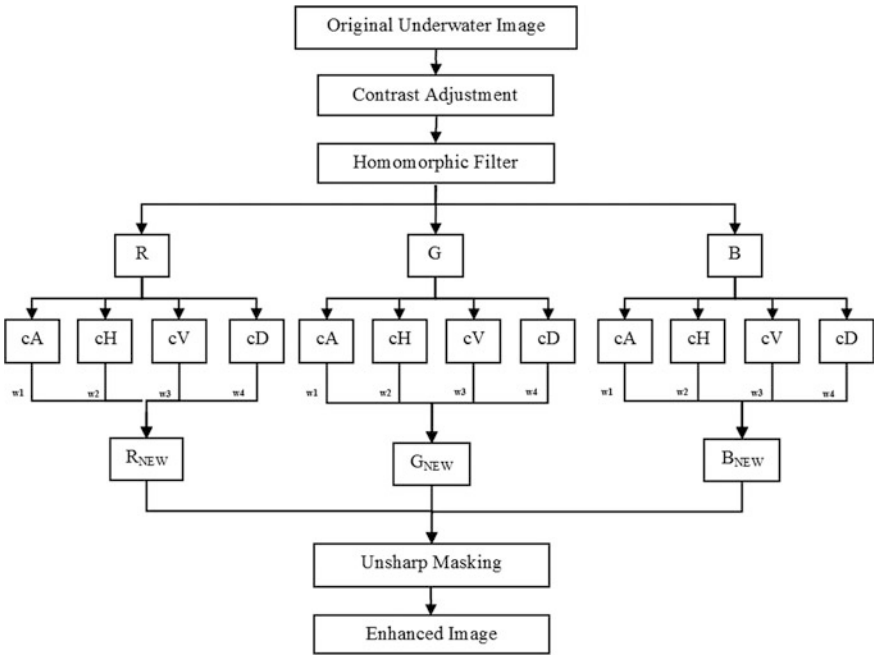

Fig. 11.5 A detailed solution flow of the proposed enhancement approach

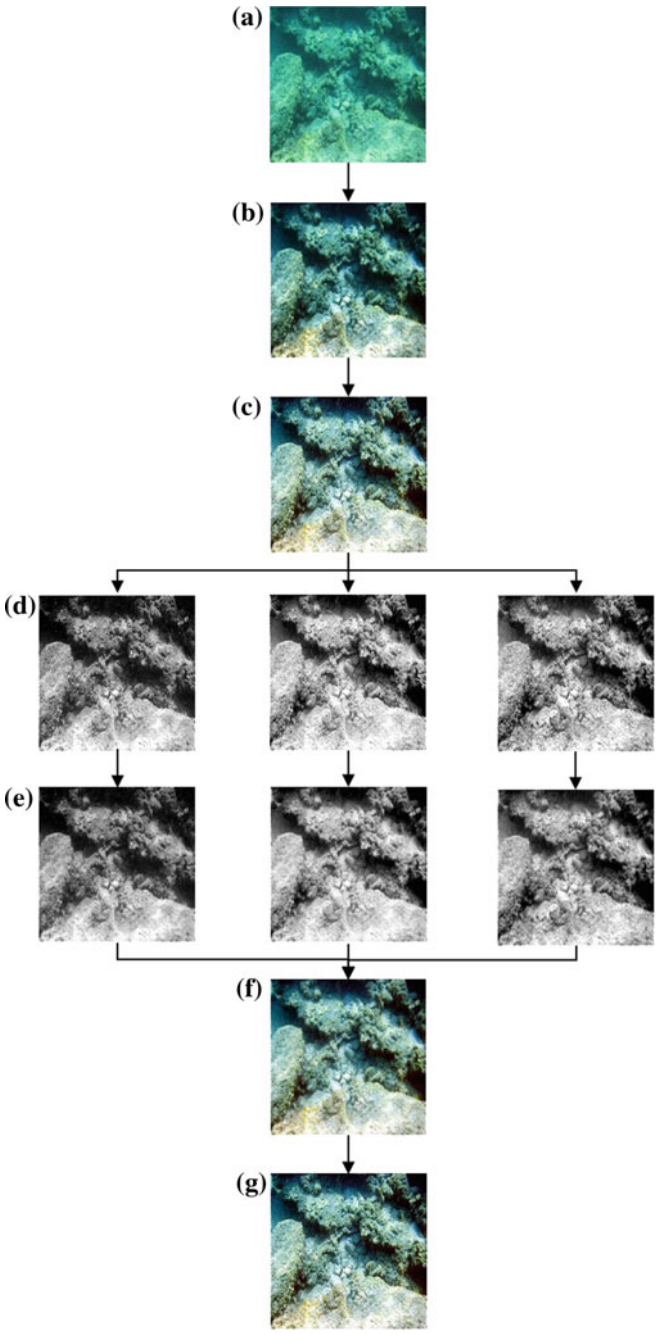

Fig. 11.6 An example process for an image by the proposed enhancement approach

11.4 Applications with the Proposed Approach

In Figs. 11.7, 11.8 and 11.9, there are some examples of the original underwater images and the enhanced underwater images using the proposed methods with the histograms. The underwater images which are image 2, image 6, image 7 and image 8 were collected from Antalya city in Turkey. Image 9 was taken from the publication written by Celebi and Erturk [58]. Image 1, image 3, image 4 and image 5 were taken from the publication written by Ghani and Isa [59].

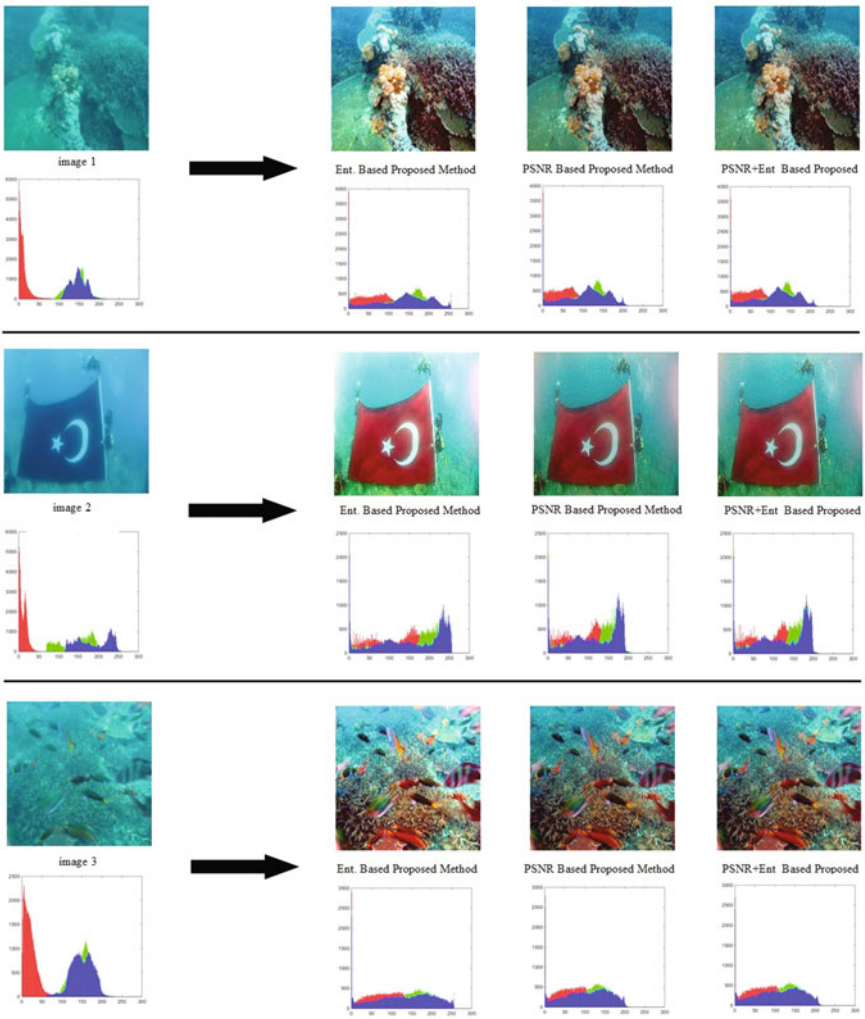

Fig. 11.7 Examples of original underwater images and enhanced underwater images with histograms (image 1, image 2, and image 3)

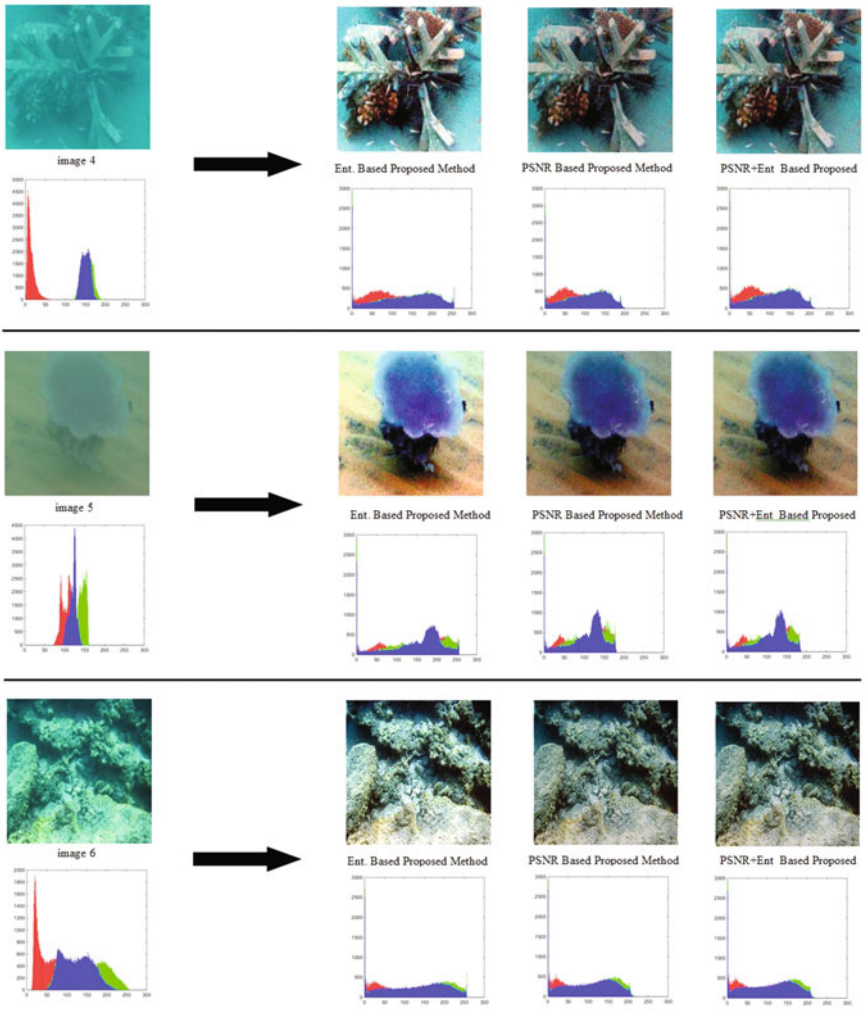

Fig. 11.8 Examples of original underwater images and enhanced underwater images with histograms (image 4, image 5, and image 6)

11.5 Evaluation

As we mentioned before, the proposed method was carried out in three different ways (in terms of comparison with the other studies in the literature) with the entropy value of the reconstructed image, PSNR value of the reconstructed image, and the sum of entropy and the PSNR value of the reconstructed image used for the information about the clarity of the image. The PSNR (Peak Signal to Noise Ratio) is known as the ratio between maximum possible power and corrupting noise that

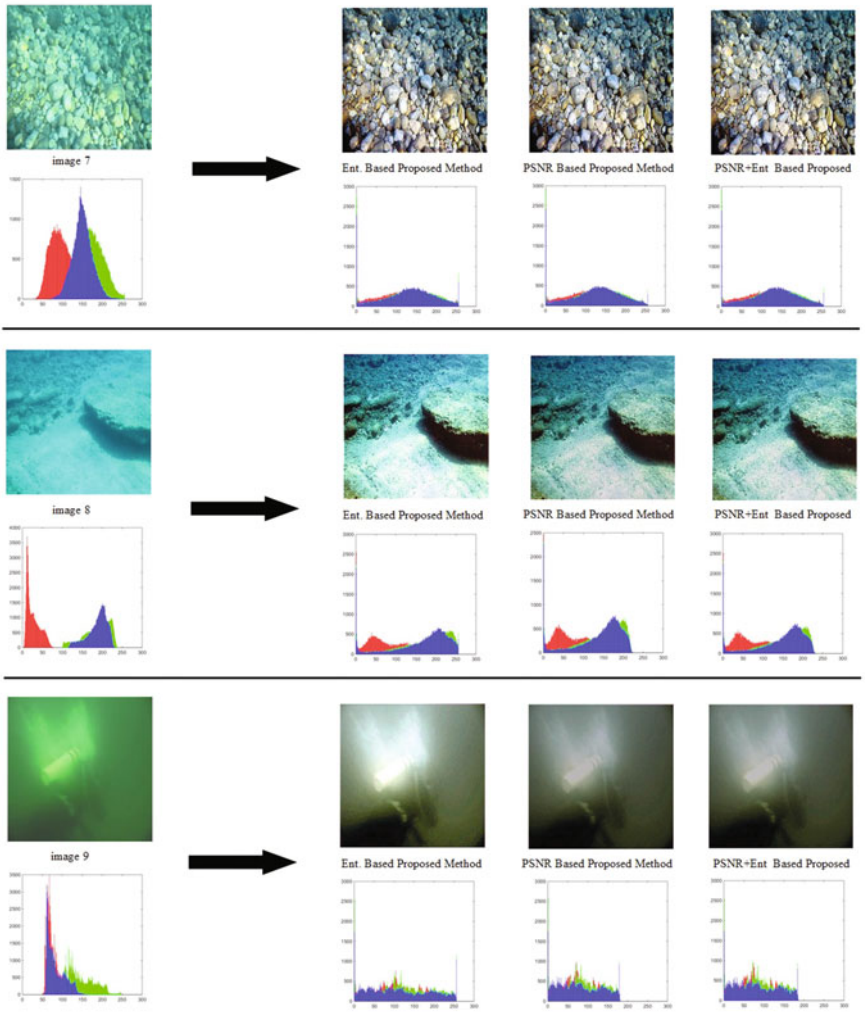

Fig. 11.9 Examples of original underwater images and enhanced underwater images with histograms (image 7, image 8, and image 9)

affect representation of an image [60]. Both PSNR and MSE are commonly used for the reconstructed or enhanced image quality measurement [60–65].

During the evaluation process, six images shown as application examples in Fig. 11.5 were considered. Regarding the evaluation, the results are given in Table 11.1 for proposed methods with PSNR, entropy, and the sum of both of them respectively. As seen in Table 11.1, proposed method with PSNR gives the best results in terms of PSNR and MSE. On the other hand, the proposed method with entropy gives the best results in terms of entropy of the final enhanced images, and

the third method with the sum of the entropy and PSNR give the best result in term of the sum of the entropy and PSNR values of the final enhanced images.

For image 6, the entropy, average gradient, and PSNR values for the proposed method and previous study performed by Guraksin et al. [66] are given in Table 11.2. Beside this, the final enhanced images mentioned in Table 11.2 are given in Fig. 11.10.

As shown in Table 11.2, there are three results of the proposed method. In the first approach, we used the proposed method considering only the entropy while calculating the weights with the differential evaluation algorithm. In the second approach, we used the proposed method with considering the PSNR value while calculating the weights with the differential evaluation algorithm. Finally, in the third approach, we used the proposed method with considering the sum of the entropy and the PSNR together while calculating the weights with the differential evaluation algorithm.

As seen from Table 11.2, all the entropy values of proposed approaches are higher than the method performed by Guraksin et al. [66]. Only the average gradient value in the approach of [66] is higher. On the other hand, the PSNR and MSE values of the proposed approaches are higher than the approach of [66]. So it can be said that the proposed approaches are more efficient than the approach performed by Guraksin et al. [66]. The differences can be seen in Fig. 11.10 (final enhanced images for image 11.6).

As seen in Fig. 11.10, all details are more distinguishable in the proposed method besides the original image and the enhanced image performed by Guraksin et al. [66]. If we examine the results of its own among the three methods performed in this study, we can see that the luminosity of the entropy based approach was higher than the PSNR and the sum of the entropy and the PSNR based approaches. Besides this, we can see that the luminosity of the PSNR based approach was lower than the entropy based and the sum of the entropy and the PSNR based approaches. The sum of the entropy and the PSNR based approaches had the luminosity between these two approaches.

It is possible to focus on more comparisons for other images. For image 11.9, the comparison of entropy values for the proposed method and previous studies performed by Celebi and Erturk [58] and Bazeille et al. [20] are given in Table 11.3. As seen from the Table 11.3, the proposed approach provides the best performance while considering the entropy value.

For images 1, 3, 4, and 5, the comparison of Entropy, PSNR, and MSE values for the proposed methods and previous studies performed by Ghani and Isa [59] are given in Table 11.4. As seen from Table 11.4, the proposed approach with entropy provides the best performance while considering the entropy values except image 5. As in image 5, the entropy value of the proposed method is close to the proposed method performed by Ghani and Isa [59]. Again, the proposed approaches with PSNR and the sum of the entropy and the PSNR together provide the best performance while considering the PSNR and MSE values of the enhanced images.

Table 11.1 The entropy, average gradient, PSNR and MSE values for the related underwater images

	Image	Entropy of the original image	Entropy of the enhanced image	Average gradient of the original image	Average gradient of the enhanced image	PSNR	MSE	Entropy of the enhanced image/ entropy of the original image	PSNR + entropy of the enhanced image/ entropy of the original image
Proposed approach with PSNR	Image 1	6.877	7.509	2.490	9.702	13.349	3007.345	1.092	3.033
	Image 2	7.416	7.490	1.481	4.624	11.569	4530.522	1.010	2.570
	Image 3	7.295	7.535	3.645	11.268	12.958	3290.589	1.033	2.809
	Image 4	6.341	7.486	1.589	8.636	11.789	4307.589	1.181	3.040
	Image 5	6.216	7.277	0.647	3.850	14.949	2080.646	1.171	3.576
	Image 6	7.694	7.614	7.236	13.694	16.613	1418.243	0.990	3.149
	Image 7	7.414	7.768	7.524	21.488	14.363	2381.117	1.048	2.985
	Image 8	7.323	7.605	3.224	10.385	12.078	4029.998	1.039	2.688
	Image 9	6.810	7.375	0.713	2.084	16.612	1418.553	1.083	3.522
Proposed approach with entropy	Image 1	6.877	7.813	2.490	12.038	12.324	3808.087	1.136	2.928
	Image 2	7.416	7.861	1.4811	5.968	10.221	6179.940	1.060	2.438
	Image 3	7.295	7.857	3.645	14.070	11.849	4247.781	1.077	2.701
	Image 4	6.341	7.868	1.589	11.329	10.686	5551.847	1.241	2.926
	Image 5	6.216	7.770	0.647	5.442	11.517	4585.775	1.250	3.103
	Image 6	7.694	7.899	7.236	16.109	14.484	2315.596	1.027	2.909
	Image 7	7.414	7.794	7.524	21.612	14.121	2517.627	1.051	2.956
	Image 8	7.323	7.814	3.2243	12.016	11.460	4646.978	1.067	2.632
	Image 9	6.810	7.860	0.713	2.961	13.037	3231.301	1.154	3.069

(continued)

Table 11.1 (continued)

	Image	Entropy of the original image	Entropy of the enhanced image	Average gradient of the original image	Average gradient of the enhanced image	PSNR	MSE	Entropy of the enhanced image/ entropy of the original image	PSNR + entropy of the enhanced image/ entropy of the original image
Proposed approach with entropy + PSNR	Image 1	6.877	7.565	2.490	10.014	13.323	3025.604	1.100	3.037
	Image 2	7.416	7.543	1.481	4.764	11.548	4553.018	1.017	2.574
	Image 3	7.295	7.590	3.645	11.651	12.932	3310.688	1.040	2.813
	Image 4	6.341	7.575	1.589	9.072	11.749	4346.942	1.195	3.047
	Image 5	6.216	7.315	0.647	3.945	14.929	2090.136	1.177	3.579
	Image 6	7.694	7.635	7.236	13.835	16.601	1422.414	0.992	3.150
	Image 7	7.414	7.777	7.524	21.600	14.358	2383.720	1.049	2.986
	Image 8	7.323	7.634	3.224	10.834	12.050	4055.867	1.043	2.688
	Image 9	6.810	7.413	0.713	2.086	16.593	1424.870	1.089	3.525

Table 11.2 The entropy, average gradient, PSNR and MSE values for image 11.6

	Entropy	Average gradient	PSNR	MSE
Original Image	7.694	7.236	–	
Guraksin et al. [66]	6.897	**19.258**	12.569	3599.183
Proposed approach with entropy	**7.899**	16.109	14.484	2315.596
Proposed approach with PSNR	7.614	13.694	**16.613**	**1418.243**
Proposed approach with PSNR + Ent	7.635	13.835	16.601	1422.414

Best values in bold

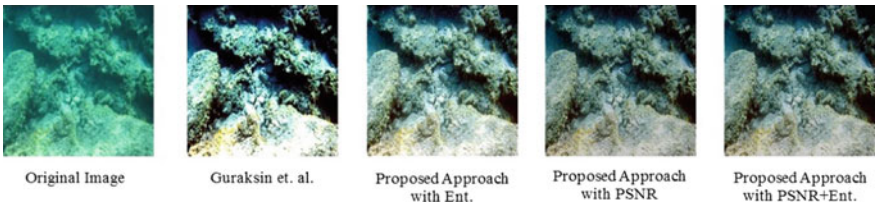

Fig. 11.10 The final enhanced images for image 6

Table 11.3 The entropy and average gradient values of other studies and entropy based proposed approach for image 11.9

Celebi and Erturk [58]	Bazeille et al. [20]	Proposed approach with entropy
Entropy of the original image = 6.19	Entropy of the original image = 6.19	Entropy of the original image = 6.81
Entropy of the enhanced image = 6.66	Entropy of the enhanced image = 6.98	Entropy of the enhanced image = 7.86
Entropy of the enhanced image/entropy of the original image = 1.100	**Entropy of enhanced the image/entropy of the original image = 1.128**	**Entropy of the enhanced image/entropy of the original image = 1.154**
Average grad. of the orig. image = 0.96	Average grad. of the orig. image = 0.96	Average grad. of the orig. image = 0.71
Average gradient of the enhanced image = 5.84	Average gradient of the enhanced image = 1.62	Average gradient of the enhanced image = 2.96
Average gradient of the enhanced image/average gradient of the original image = 6.08	**Average gradient of the enhanced image/average gradient of the original image = 1.69**	**Average gradient of the enhanced image/average gradient of the original image = 4.17**

Table 11.4 Entropy, PSNR, and MSE values for the image 1, image 3, image 4 and image 5

		Entropy (original)	Entropy (enhanced)	PSNR	MSE	Ent. Enh./Ent Org.	PSNR + Ent Enh./Ent. Org.
Image 1	Ghani and Isa [59]	6.902	7.702	12.33	3801	1.116	2.902
	Prop.App (Ent.)	6.877	7.813	12.32	3808	**1.136**	2.928
	Prop.App (PSNR)	6.877	7.509	**13.35**	**3007**	1.092	3.033
	Prop.App (PSNR + Ent)	6.877	7.565	13.32	3026	1.100	**3.037**
Image 3	Ghani and Isa [59]	7.341	7.764	12.79	3424	1.058	2.800
	Prop.App (Ent.)	7.295	7.857	11.85	4248	**1.077**	2.701
	Prop.App (PSNR)	7.295	7.535	**12.96**	**3291**	1.033	2.809
	Prop.App (PSNR + Ent)	7.295	7.590	12.93	3311	1.040	**2.813**
Image 4	Ghani and Isa [59]	6.341	7.866	10.87	5317	1.240	2.955
	Prop.App (Ent.)	6.341	7.868	10.69	5552	**1.241**	2.926
	Prop.App (PSNR)	6.341	7.486	**11.79**	**4308**	1.181	3.040
	Prop.App (PSNR + Ent)	6.341	7.575	11.75	4347	1.195	**3.047**
Image 5	Ghani and Isa [59]	6.218	7.857	13.15	3149	**1.264**	3.378
	Prop.App (Ent.)	6.216	7.770	11.52	4586	1.250	3.103
	Prop.App (PSNR)	6.216	7.277	**14.95**	**2081**	1.171	3.576
	Prop.App (PSNR + Ent)	6.216	7.315	14.93	2090	1.177	**3.579**

Best values in bold

11.6 Conclusions and Future Work

Underwater images have poor contrast and resolution. So enhancement of underwater images has a significant role due to the absorption and scattering of light in underwater environment. In this paper, we proposed a new approach to enhance underwater images using the wavelet transform and differential evolution algorithm. At first, some preprocessing operations like contrast adjustment and homomorphic filtering operations were performed to the raw underwater images. Then image was

separated into its R, G, and B color components. After that, by the help of wavelet transform, lowpass approximation (cA), horizontal (cH), vertical (cV) and diagonal (cD) detailed images were obtained for each color channels, and weighting procedure was applied to these color channels obtained using the differential evaluation algorithm. After that, weighted R, G, and B components was fused, and the new color image was obtained. At the last step, unsharp masking procedure was applied to the new color image and the enhanced version of the underwater image was obtained. During the weighting procedure, the proposed method was carried out in three different ways with the entropy value of the reconstructed image, PSNR value of the reconstructed image and the sum of entropy and the PSNR value of the reconstructed image. First of all, the enhanced images were examined using the proposed method with these three attributes used for the information about the clarity of the image.

According to the results obtained, all details were more distinguishable in the proposed method besides the original image and the enhanced image. If we examine the results of its own among the three methods performed in this study, we can see that the luminosity of the entropy based approach was higher than the PSNR and the sum of the entropy and the PSNR based approaches. Therefore, some details in the image could not be seen properly. Besides this, we can see that the luminosity of PSNR based approach was lower than the entropy based and the sum of the entropy and the PSNR based approaches. So this caused the image to be a little darker which was an unwanted situation. The sum of the entropy and the PSNR based approaches had the luminosity between these two approaches. Consequently, in our opinion, the sum of the entropy and the PSNR based approaches was more efficient than the entropy based and PSNR based approaches. In this study, the proposed method was used on different underwater images, and the results were compared with the other studies in the related literature in terms of entropy and PSNR. According to the obtained results, it can be said that the proposed approach effectively improved the visibility of underwater images.

In addition to the performed studies, the authors are also focused on some future researches. In this context, there will be some researches on applying the proposed approach in different underwater conditions and different places to have more and more ideas about success of the approach. On the other hand, different variations of the approach, which are formed with the support of different optimization algorithms, will be applied to the same research problem to see if it is possible to have alternative solution ways for the related literature.

Acknowledgements This paper has been supported by Afyon Kocatepe University Scientific Research and Projects Unit with the Project number 16.KARİYER.46. The authors also would like to thank to Ali Topal for his support to adapt the study content to Springer chapter requirements.

References

1. Chiang, J.Y., Chen, Y.C.: Underwater image enhancement by wavelength compensation and dehazing. IEEE Trans. Image Process. **21**(4), 1756–1769 (2012)
2. Jayasree, M.S., Thavaseelan, G.: Underwater color image enhancement using wavelength compensation and dehazing. Int. J. Comput. Sci. Eng. Commun. **2**(3), 389–393 (2014)
3. Kaur, T., Sidhu, R.K.: Performance evaluation of fuzzy and histogram based color image enhancement. Proc. Comput. Sci. **58**, 470–477 (2015)
4. Lakshmi, R.S., Loganathan, B.: An efficient underwater image enhancement using color constancy deskewing algorithm. Int. J. Innovative Res. Comput. Commun. Eng. **3**(8), 7164–7168 (2015)
5. Lathamani, K.M., Maik, V.: Blur analysis and removal in underwater images using optical priors. Int. J. Emerg. Technol. Adv. Eng. **5**(2), 59–65 (2015)
6. Torres-Méndez, L.A., Dudek, G.: Color correction of underwater images for aquatic robot inspection. In: International Workshop on Energy Minimization Methods in Computer Vision and Pattern Recognition, pp. 60–73. Springer, Berlin (2005)
7. Prabhakar, C.J., Praveen Kumar, P.U.: An image based technique for enhancement of underwater images. Int. J. Mach. Intell. **3**(4), 217–224 (2011)
8. Banerjee, J., Ray, R., Vadali, S.R.K., Shome, S.N., Nandy, S.: Real-time underwater image enhancement: an improved approach for imaging with AUV-150. Sadhana **41**(2), 225–238 (2016)
9. Farhadifard, F., Zhou, Z., von Lukas, U.F.: Learning-based underwater image enhancement with adaptive color mapping. In: 2015 9th International Symposium on Image and Signal Processing and Analysis (ISPA), pp. 48–53. IEEE (2015)
10. Ghani, A.S.A., Aris, R.S.N.A.R., Zain, M.L.M.: Unsupervised contrast correction for underwater image quality enhancement through integrated-intensity stretched-rayleigh histograms. J. Telecommun. Electr. Comput. Eng. **8**(3), 1–7 (2016)
11. Hitam, M.S., Awalludin, E.A., Yussof, W.N.J.H.W., Bachok, Z.: Mixture contrast limited adaptive histogram equalization for underwater image enhancement. In: 2013 International Conference on Computer Applications Technology (ICCAT), pp. 1–5. IEEE
12. Li, X., Yang, Z., Shang, M., Hao, J.: Underwater image enhancement via dark channel prior and luminance adjustment. In: OCEANS 2016-Shanghai, pp. 1–5. IEEE (2016)
13. Lu, H., Li, Y., Xu, X., Li, J., Liu, Z., Li, X., et al.: Underwater image enhancement method using weighted guided trigonometric filtering and artificial light correction. J. Vis. Commun. Image Represent. **38**, 504–516 (2016)
14. Sethi, R., Sreedevi, I., Verma, O.P., Jain, V.: An optimal underwater image enhancement based on fuzzy gray world algorithm and bacterial foraging algorithm. In: 2015 Fifth National Conference on Computer Vision, Pattern Recognition, Image Processing and Graphics (NCVPRIPG), pp. 1–4. IEEE (2015)
15. Sheng, M., Pang, Y., Wan, L., Huang, H.: Underwater images enhancement using multi-wavelet transform and median filter. Indonesian J. Electr. Eng. Comput. Sci. **12**(3), 2306–2313 (2014)
16. Beohar, R., Sahu, P.: Performance analysis of underwater image enhancement with CLAHE 2D median filtering technique on the basis of SNR, RMS error, mean brightness. Int. J. Eng. Innovative Technol. **3** (2013)
17. Eustice, R., Pizarro, O., Singh, H., Howland, J.: UWIT: underwater image toolbox for optical image processing and mosaicking in MATLAB. In: Proceedings of the 2002 International Symposium on Underwater Technology, 2002, pp. 141–145. IEEE (2002)
18. Haile, M.A., Yin, W., Ifju, P.G.: MATLAB® based image preprocessing and digital image correlation of objects in liquid. In: SEM Annual Conference & Exposition on Experimental and Applied Mechanics, pp. 1–11 (2009)
19. Serikawa, S., Lu, H.: Underwater image dehazing using joint trilateral filter. Comput. Electr. Eng. **40**(1), 41–50 (2014)

20. Bazeille, S., Quidu, I., Jaulin, L., Malkasse, J.-P.: Automatic underwater image pre-processing. In: CMM'06, Brest, France (2006).
21. Kose, U., Guraksin, G.E., Deperlioglu, O.: Improving underwater image quality via vortex optimization algorithm. In: International Multidisciplinary Conference IMUCO '16, 21–22 April 2016, Antalya, Turkey, pp. 327–333 (2016)
22. Preethi, S.J., Rajeswari, K.: Membership function modification for image enhancement using fuzzy logic. Int. J. Emerging Trends Technol. Comput. Sci. **2**(2), 115–118 (2013)
23. Babu, R.K., Sunitha, K.V.N.: Enhancing digital images through cuckoo search algorithm in combination with morphological operation. J. Comput. Sci. **11**(1), 7–17 (2015)
24. Li, Q.Z., Wang, W.J.: Low-bit-rate coding of underwater color image using improved wavelet difference reduction. J. Vis. Commun. Image Represent. **21**(7), 762–769 (2010)
25. Porwik, P., Lisowska, A.: The Haar-wavelet transform in digital image processing: its status and achievements. Mach. Graphic. Vis. **13**(1/2), 79–98 (2004)
26. Das, S., Suganthan, P.N.: Differential evolution: a survey of the state-of-the-art. IEEE Trans. Evol. Comput. **15**(1), 4–31 (2011)
27. Neri, F., Tirronen, V.: Recent advances in differential evolution: a survey and experimental analysis. Artif. Intell. Rev. **33**(1–2), 61–106 (2010)
28. Price, K., Storn, R.M., Lampinen, J.A.: Differential Evolution: A Practical Approach to Global Optimization. Springer Science & Business Media, Heidelberg (2006)
29. Addison, P.S.: The Illustrated Wavelet Transform Handbook: Introductory Theory and Applications in Science, Engineering, Medicine and Finance. CRC Press, Boca Raton (2017)
30. Sifuzzaman, M., Islam, M.R., Ali, M.Z.: Application of wavelet transform and its advantages compared to fourier transform. J. Phys. Sci. **13**, 121–134 (2009)
31. Sharma, M., Singh, G., Gupta, R.: Application of wavelet–an advanced approach of transformation. Adv. Res. Electr. Electron. Eng. **1**(1), 28–34 (2014)
32. Misiti, M., Misiti, Y., Oppenheim, G., Poggi, J.-M.: Wavelet Toolbox™ Reference. The MathWorks, Inc., Natick (2016)
33. Mallat, S.G.: A theory for multiresolution signal decomposition: the wavelet representation. IEEE Trans. Pattern Anal. Mach. Intell. **11**(7), 674–693 (1989)
34. Storn, R., Price, K.: Differential Evolution—A Simple and Efficient Adaptive Scheme for Global Optimization Over Continuous Spaces, vol. 3. ICSI, Berkeley (1995)
35. Storn, R., Price, K.: Differential evolution—a simple and efficient heuristic for global optimization over continuous spaces. J. Glob. Optim. **11**(4), 341–359 (1997)
36. Chen, S., Rangaiah, G.P., Srinivas, M.: Differential evolution: method, developments and chemical engineering applications. Diff. Evol. Chem. Eng. Dev. Appl. **6**, 35 (2017)
37. Chakraborty, U.K. (ed.): Advances in Differential Evolution, vol. 143. Springer, Heidelberg (2008)
38. El Ela, A.A., Abido, M.A., Spea, S.R.: Optimal power flow using differential evolution algorithm. Electr. Power Syst. Res. **80**(7), 878–885 (2010)
39. Wang, L., Zeng, Y., Chen, T.: Back propagation neural network with adaptive differential evolution algorithm for time series forecasting. Expert Syst. Appl. **42**(2), 855–863 (2015)
40. Penas, D.R., Banga, J.R., González, P., Doallo, R.: Enhanced parallel differential evolution algorithm for problems in computational systems biology. Appl. Soft Comput. **33**, 86–99 (2015)
41. Augusteen, W.A., Kumari, R., Rengaraj, R.: Economic and various emission dispatch using differential evolution algorithm. In: 2016 3rd International Conference on Electrical Energy Systems (ICEES), pp. 74–78. IEEE (2016)
42. Bas, E.: The training of multiplicative neuron model based artificial neural networks with differential evolution algorithm for forecasting. J. Artif. Intell. Soft Comput. Res. **6**(1), 5–11 (2016)
43. Fan, H.Y., Lampinen, J.: A trigonometric mutation operation to differential evolution. J. Global Optim. **27**(1), 105–129 (2003)
44. Mayer, D.G., Kinghorn, B.P., Archer, A.A.: Differential evolution–an easy and efficient evolutionary algorithm for model optimisation. Agric. Syst. **83**(3), 315–328 (2005)

45. Vesterstrom, J., Thomsen, R.: A comparative study of differential evolution, particle swarm optimization, and evolutionary algorithms on numerical benchmark problems. In: CEC2004. Congress on Evolutionary Computation, 2004, vol. 2, pp. 1980–1987. IEEE (2004)
46. Khan, S.U., Qureshi, I.M., Zaman, F., Shoaib, B., Naveed, A., Basit, A.: Correction of faulty sensors in phased array radars using symmetrical sensor failure technique and cultural algorithm with differential evolution. Sci. World J. (2014)
47. Brownlee, J.: Differential evolution. Clever algorithms: nature-inspired programming recipes. http://www.cleveralgorithms.com/nature-inspired/evolution/differential_evolution.html. Retrieved 25 Sept 2016 (2016)
48. Cortés-Antonio, P., González, J.R., Villa-Vargas, L.A., Ramırez-Salinas, M.A., Molina-Lozano, H., Batyrshin, I.: Design and implementation of differential evolution algorithm on FPGA for double-precision floating-point representation. Acta Polytech. Hung. **11**(4), 139–153 (2014)
49. Sumithra, S., Victoire, T.: Differential evolution algorithm with diversified vicinity operator for optimal routing and clustering of energy efficient wireless sensor networks. Sci. World J. (2015)
50. Liu, J., Lampinen, J.: A fuzzy adaptive differential evolution algorithm. Soft. Comput. **9**(6), 448–462 (2005)
51. Abbass, H.A.: The self-adaptive Pareto differential evolution algorithm. In: Proceedings of the 2002 Congress on Evolutionary Computation, 2002. CEC'02, vol. 1, pp. 831–836. IEEE (2002)
52. Chaturvedi, P., Kumar, P.: Population segmentation-based variant of differential evolution algorithm. In: Proceedings of Fifth International Conference on Soft Computing for Problem Solving, pp. 401–410. Springer, Singapore (2016)
53. Sayah, S., Zehar, K.: Modified differential evolution algorithm for optimal power flow with non-smooth cost functions. Energy Convers. Manag. **49**(11), 3036–3042 (2008)
54. Mallipeddi, R., Lee, M.: An evolving surrogate model-based differential evolution algorithm. Appl. Soft Comput. **34**, 770–787 (2015)
55. Wazir, H., Jan, M.A., Mashwani, W.K., Shah, T.T.: A penalty function based differential evolution algorithm for constrained optimization. Nucleus **53**(2), 155–161 (2016)
56. Zhang, J., Lin, S., Qiu, W.: A modified chaotic differential evolution algorithm for short-term optimal hydrothermal scheduling. Int. J. Electr. Power Energy Syst. **65**, 159–168 (2015)
57. Solomon, C., Breckon, T.: Fundamentals of Digital Image Processing. Wiley-Blackwell, West Sussex (2011)
58. Celebi, A.T., Erturk, S.: Visual enhancement of underwater images using emprical mode decomposition. Expert Syst. Appl. **39**, 800–805 (2012)
59. Ghani, A.S.A., Isa, N.A.M.: Underwater image quality enhancement through composition of dual-intensity images and Rayleigh-stretching. SpringerPlus **3**(1), 1–14 (2014)
60. Kaushik, P., Sharma, Y.: Comparison of different image enhancement techniques based upon PSNR & MSE. Int. J. Appl. Eng. Res. **7**(11), 2010–2014 (2012)
61. Grgic, S., Grgic, M., Mrak, M.: Reliability of objective picture quality measures. J. Electr. Eng. **55**(1–2), 3–10 (2004)
62. Huang, X.Q., Shi, J.S., Yang, J., Yao, J.C.: Study on color image quality evaluation by MSE and PSNR based on color difference. Acta Photonica Sin. **36**(8), 295–298 (2007)
63. Kipli, K., Muhammad, M., Masra, S., Zamhari, N., Lias, K., Azra, D.: Performance of Levenberg-Marquardt backpropagation for full reference hybrid image quality metrics. In: Proceedings of International Conference of Multi-Conference of Engineers and Computer Scientists (IMECS'12) (2012)
64. Wang, Z., Bovik, A.C.: A universal image quality index. IEEE Signal Process. Lett. **9**(3), 81–84 (2002)
65. Wang, Z., Bovik, A.C., Sheikh, H.R., Simoncelli, E.P.: Image quality assessment: from error visibility to structural similarity. IEEE Trans. Image Process. **13**(4), 600–612 (2004)
66. Guraksin, G.E., Kose, U., Deperlioglu, O.: Underwater image enhancement based on contrast adjustment via differential evolution algorithm. In: 2016 International Symposium on INnovations in Intelligent SysTems and Applications (INISTA), pp. 1–5. IEEE (2016)